Experimental evaluation of the thermal conductivity for additive manufactured materials. New test facility concept and preliminary tests

N Bianco[1], R Mastrullo[1], A W Mauro[1] and L Viscito[1*]

[1] Department of Industrial Engineering, Federico II University of Naples, P.le Tecchio 80, 80125 Naples (Italy)

*Corresponding author e-mail: luca.viscito@unina.it

Abstract. Items for heat transfer made by metal foams or additive manufactured structures allow to create special components for several applications (i.e. fast response PCM, complex and light HEXs working at high temperatures for the aerospace sector). For their design thermo-physical properties data are required, such as thermal conductivity. To accurately measure this parameter with conventional procedures for metallic items (e.g. flash methods), the specific heat and density should be measured each time depending on the actual composition of the porous media (estimation is not yet reliable and porosity not known). The scope of this paper is to validate a test facility and the relative method for the data reduction to proof the possibility to measure directly the thermal conductivity with samples of small size. The experiments, carried-out with square samples (30×30 mm^2), allow to measure a range of thermal conductivity between 5 and 50 W/m K. The main aspect of the experimental method is the calibration of the heat losses towards the environment by means of a reverse technique. The assessment of the results against samples of known materials was good.

Keywords: *thermal conductivity, test facility concept, additive manufacturing, UHTC materials*

1. Introduction

In the last decades, it has become necessary to develop and produce geometrically complex items for any kind of application. It is indeed important for the industrial sector to exploit new production technologies aimed at the realization of innovative materials having more and more performing mechanical and thermophysical properties. On this regard, the advent of 3-D printers has opened complete new scenarios and great importance was attributed to the Additive Manufacturing (AM). This technique largely differs from conventional items production processes, typically based on metals melting or on chip-cutting machining that realize the desired object from a single block. The new AM technique relies instead on a "layer-by-layer" procedure, consisting in the deposition of material in thin layers, one above the others, in the form of metal wires, powders or liquids, catching the final CAD-made 3-D sketch of the desired item. 3-D printing is already moving from a purely prototype technology to an end-use manufacturing process. As a fact, the AM technique is becoming widely known since the costs related to using 3-D printers have significantly decreased over the last years, allowing more and more people and companies to have access to this technology [1]. Some examples can be given through the exploitation of AM in creating replacement parts for old equipment, molds and tools able to assist in manufacturing other products, and also the realization of brand new products that take advantage of

the unique peculiarities allowed by AM. For instance, each layer can be made of a different material thus having very heterogeneous combinations, with singular physical and mechanical characteristics, exploitable in the biomedical field. Moreover, very complex geometries such as high efficiency heat exchangers for aerospace applications can be easily realized by using AM [2], thus reducing weight and limiting the number of individual components and connecting tools/bolts to assemble the final item.

However, one major drawback of the AM technology is the complex determination of the material properties [3], since the final product is neither homogeneous nor isotropic, but is rather considered an anisotropic porous material with micro air bubbles randomly placed inside the object [4]. This characteristic reflects on the evaluation of crucial thermophysical properties, such as the specific heat and thermal conductivity, especially in case of heat exchangers or other thermal duty applications.

The determination of the thermal conductivity is a key aspect also for other innovative materials, such as Ultra-High Temperature Ceramics (UHTCs) employed in atmospheric entry operation of outer space elements. The evaluation of the thermal conductivity for these porous materials at high temperature is usually carried-out by employing difficult mathematical models [5], whereas on-field tests are not performed due to the lack of a proper available method.

Conventional available methods aimed at the evaluation of the thermal conductivity are unsuitable for the abovementioned materials, and usually consist in steady state one dimensional experiments ("Hot plate" procedure) or transient conduction tests ("Flash method"). In fact, the hot plate procedure generally requires very large samples and is applied for light building insulating materials (thermal conductivities less than 0.1 W/m K). The flash method is instead an indirect procedure and allows the calculation of the thermal diffusivity, thus requiring the knowledge of the material density and specific heat, usually unknown for heterogeneous and porous materials.

For this reason, a heat conduction apparatus was specifically designed in this study to perform experiments on materials in order to evaluate their thermal conductivity, within the range of 5-50 W/mK, expected for AM and ceramic items, and temperatures up to 150 °C. The heat losses and the contact thermal resistance of the samples were also characterized to enhance the accuracy of the results shown. The set-up of the test facility was performed by using stainless steel (AISI-304L type), obtaining a good agreement between experimental and provided thermal conductivity data.

2. Experimental facility

2.1. Test section and concept

The sketch and a photograph of the test facility is shown in Figure 1. The test rig concept is similar to that conceived by Flaata et al. [6], proposing some modification related to the heating method and the geometrical arrangement. It consists of a copper hot plate and a cold copper plate (390 W/m K) separated by the specimen material, having a square cross section of 30x30 mm^2. The heat is provided by Joule effect thanks to a ceramic heater (Bach RC GmbH, customized), which is placed in a dedicated slot carved in the hot copper block. The variable power supply is given by a DC power unit with a capacity of 0-10 A and 0-40 V, by controlling the voltage value. A water multi-minichannel heat sink is obtained at the edge of the cold copper block to cool down the test section. Both cold and hot blocks are then connected to a mica block material (0.72 W/mK), a wood square block and a screwing system able to tighten the whole structure. In order to avoid undesired relative rotations, two copper linchpins (1.5 mm deep) are provided for each side of the specimen as connecting elements between the sample and the copper blocks. The negligible alteration of the 1-D temperature field was verified with previous simulations. Both copper blocks and the tested specimens were accurately polished before the set-up operations, in order to obtain the best possible adherence between the surfaces. Moreover, a thermal compound (3.2 W/mK) was placed among connecting parts as a further way to improve thermal contact. Finally, four holes (diameter of 1.5 mm and 10 mm depth) are provided in the copper blocks right before and after (less than 1.0 mm) the specimen, to allow the sample temperature measurements. In order to ensure a fair estimation of the blocks temperature, all the 8 thermocouples were fastened with cyanoacrylate glue inside their slots, in which a conspicuous amount of thermal compound was also used. Other 2 T-type thermocouples are respectively placed close to the ceramic heater slot and in the environment in order to estimate the maximum temperature reached in the test facility and the ambient

temperature during experiments, thus allowing the evaluation of the heating losses. The whole test facility, horizontally arranged, was insulated with a considerable amount of synthetic foam (multiple layers for a total amount of more than 15 cm) having a thermal conductivity lower than 0.07 W/m K, to limit the heat losses to the surrounding ambient as much as possible and to corroborate the hypothesis of one dimensional heat transfer in the test section. From a preliminary analysis performed with a computational software, the hot copper block length was found to be largely sufficient to guarantee the heat flux uniformity, in the whole range of experimented operating conditions.
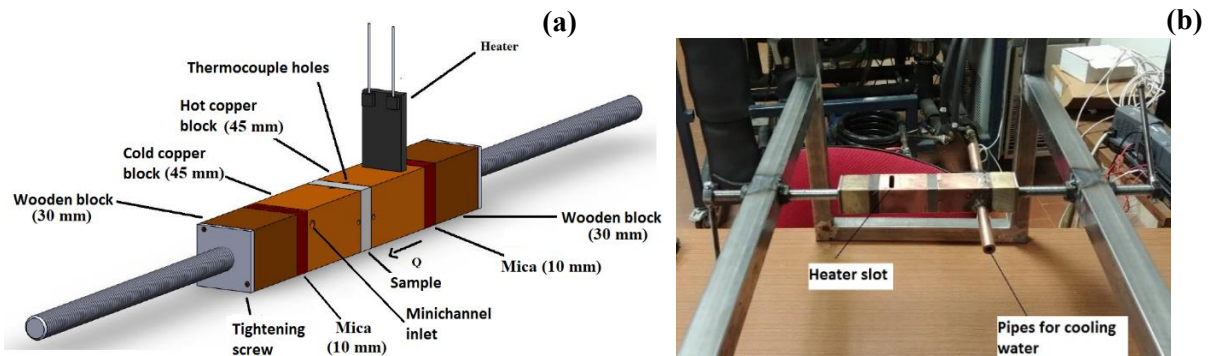

Figure 1. (a) Schematic lay-out of the test rig with all the parts exposed; (b) Photograph of the test section.

2.2. Measurement instrumentation

The temperature measurement at the specimen hot and cold edges is carried out by using eight T-type thermocouples, respectively at the top, bottom, left and right sides for each copper block, very close to the specimen section. Two additional T-type thermocouples are respectively located in the environment and close to the heating section in the hot copper block. All the thermocouples signals are read by an input voltage module that provides the desired temperature value with an overall accuracy of ±0.37 °C. The DC power supply unit gives variable voltages and currents in the range of 0-40 V and 0-10 A, respectively. The current is directly measured by the power supply unit, with an overall accuracy of ±0.2% of the reading, as stated by the manufacturer. The voltage applied to the ceramic heater is instead measured with two wires directly applied on the heater nickel terminals, in order to compensate possible voltage drops in the connecting copper wires. The voltage input module provides the measurement with an overall accuracy of ±0.52%.

3. Method

3.1. Model and measurement algorithm

A linear function of the mean temperature value reached by the specimen during the experiment is considered for the evaluation of the thermal conductivity, as shown in Equation (1):

$$\bar{k} = a + b \cdot \bar{T} \qquad (1)$$

The constants a and b are unknown and are calibrated according to a numerical model that follows an iterative procedure, which will be shown in this section. According to Figure (2), s is the sample thickness, whereas $\bar{T}_H$ and $\bar{T}_C$ represent the mean measured temperature values of the four type-T thermocouples placed before and after the sample, respectively. The thermal resistance of the copper layers between the thermocouples location and the specimen surface has been neglected thanks to the reduced distance and the very high thermal conductivity of pure copper (398 W/m K). The effective heat load crossing the specimen is the measured electric power (equal to the product between the imposed voltage and current) minus the heat losses in the hottest section close to the heater ($Q_{loss,heater}$)

and the heat losses along the specimen extension ($Q_{loss,sp}$). In this model, both hot and cold sides contact resistances, named R_H and R_C, respectively, between the specimen and copper surfaces, are also taken into account.
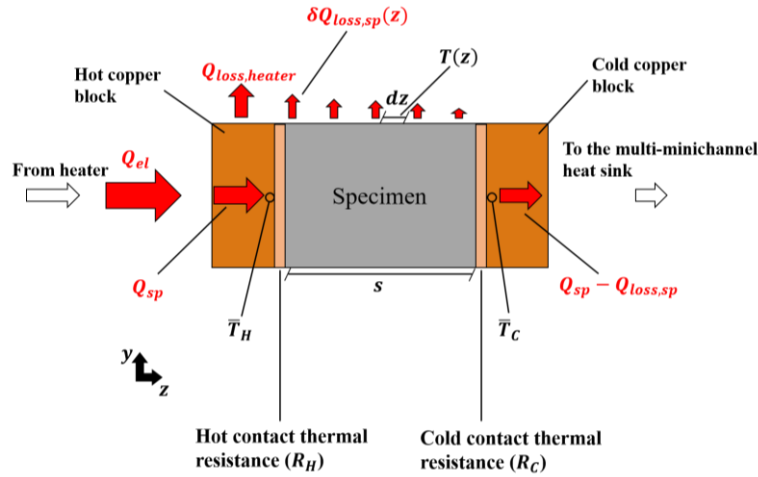

Figure 2. Model concept

The expression of the heater losses is presented in Equation (2), in which A_{heater} is the upstream area of the sample, T_{max} is the maximum measured temperature value reached during the tests from the thermocouple placed close to the heater slot and T_{amb} represents the ambient temperature value:

$$Q_{loss,heater} = U_{loss} \cdot A_{heater} \cdot (T_{max} - T_{amb}) \tag{2}$$

Therefore, the current heat load right before the beginning of the sample is represented by the difference between the electric power supplied to the specimen and the heater losses, in which z coordinate is perpendicular to the specimen surface:

$$Q_{sp} = Q(z = 0) = Q_{el} - Q_{loss,heater} \tag{3}$$

The specimen temperature value for each z-axis position is given by an energy balance on the specimen part of thickness dz:

$$T(z) = T(z - dz) - \frac{Q(z)}{A} \cdot \left(\frac{dz}{\bar{k}}\right) \tag{4}$$

The specimen cross sectional area A is obtained by multiplying the exact measured values of two sides L1xL2. For first and last elements of integration, Equation (4) also takes into account the hot R_H and cold R_C side contact resistances between the specimen and the copper surfaces. The local heat power crossing the sample is obtained by Equation (5), where the subtractive term refers to the specimen losses, which are a function of the local sample temperature and the ambient temperature.

$$Q(z) = Q_{sp} - \int_0^z U_{loss} \cdot 2 \cdot (L1 + L2) \cdot (T(z) - T_{amb}) \cdot dz \tag{5}$$

The parameters a, b, U_{loss}, R_H and R_C are unknown, so their calibration is needed. An algorithm is implemented and solved with a MATLAB code [7] and the following steps are executed:
   a)   A triplet (*i*) of the values a, b and U_{loss} is fixed;
   b)   The specimen thickness (*j*) is fixed among the available ones;
   c)   The values of R_H and R_C are chosen (*k*);

d) The cold mean temperature of the model ($\bar{T}_C$) is calculated according to the numeric integration of Equation (4);

e) For the whole set of N experiments at thickness (*j*), the error between the cold mean temperature of the model and the cold mean temperature measured by the thermocouples is evaluated, through the $RMSE(i,j,k)$ parameter, as shown in Equation (6):

$$RMSE(i,j,k) = \sqrt{\frac{\sum_{i=1}^{N}(\bar{T}_C - \bar{T}_{C,mod}(i,j,k))^2}{N}} \qquad (6)$$

f) The procedure from point c) to e) is repeated for each values of R_H and R_C: in this way is it possible to estimate the minimum value of the error at each specimen thickness:

$$minError(i,j) = \min(RMSE(i,j,k)) \qquad (7)$$

g) This procedure is repeated for any specimen thickness (*j*) and for each triplet (*i*), obtaining an array of the error sums:

$$error\_array(i) = sum(minError(i,j)) \qquad (8)$$

h) The minimum value of the array determines the triplet values of the parameters a, b and U_{loss}, from which the R_H and R_C values are finally obtained for each sample thickness.

3.2. Uncertainty analysis

The uncertainty of the measured parameters of interest was calculated by composing the instrumental accuracy to the unavoidable fluctuations observed during the experiments, corresponding to the standard deviation in the recording period. For the sample dimensions, a Vernier electronic caliper (±0.01 mm) was employed with numerous (more than 30) measurements, with the results shown in Figure 3 of paragraph 4.1. In case of derived parameters, the uncertainty was computed according to the law of propagation of errors [8]. Either case, the expanded uncertainty was finally obtained by using a coverage factor of 2, thus guaranteeing a confidence level higher than 95%. A summary of the calculated uncertainty for all the parameters of interest is given in Table 1.

Table 1. Uncertainty of the parameters of interest

Parameter	Calculated uncertainty (coverage factor = 2)
Specimen temperatures	±0.4 °C
Specimen $\Delta T = \bar{T}_H - \bar{T}_C$	±0.6 °C
Heat power	±5.9%
Thermal conductivity	±12.1%

3.3. Experimental procedure

All the tests are carried-out in steady state conditions, with a recording time and frequency of 120 s and 1 Hz, respectively. The desired heat rate across the specimen section is set by changing the DC voltage applied to the ceramic heater. A constant water flow is given for the cold copper block to set the sink temperature value. Power and temperatures values are then constantly monitored and controlled via user interface and the system is let to stabilize until steady state condition is reached. Particularly, the recording time was allowed to start only when the fluctuations of the 8 acquisition period did not exceed 0.3 °C (which is lower than the uncertainty of the measurement itself). The ambient temperature fluctuation was also controlled and limited to 0.5 °C to avoid excessive variation of the heat losses.

4. Experimental results

4.1. Samples

The purpose of these tests was to validate the model and the experimental procedure. For this reason, all experiments were carried-out by using stainless-steel (AISI 304 L), having a reference thermal

conductivity at 20 °C of around 15 W/m K, falling within the possible range of additive manufactured and ultra-high temperature ceramics materials. However, the real thermal conductivity may slightly differ from one manufacturer to another caused by minor chemical differences in the tested samples, and its value can be estimated as a function of the temperature from different reference studies according to their measurement procedure. Graves et al. [9] at the Oak Ridge National Laboratory (ORNL) obtained the following equation, in which the temperature must be inserted in [K]:

$$k_{ORNL} = 7.9318 + 0.023051 \cdot T - 6.4166 \cdot 10^{-6} \cdot T^2 \tag{9}$$

Bogaard [10] and Chu and Ho [11] also measured the thermal conductivity of AISI 304 L in the temperature range of 300-700 K. The fitting equation for Chu and Ho [11] results is given as follows:

$$k_{Chu} = 8.021 + 0.02715 \cdot T - 1.418 \cdot 10^{-5} \cdot T^2 \tag{10}$$

In the present experimental campaign, five square samples with a different thickness were cut from the same AISI 304 L (30x30 mm^2) square rod. A picture of the specimens used and their dimensions (L1xL2xs) is provided in Figure 3 and Table 2.
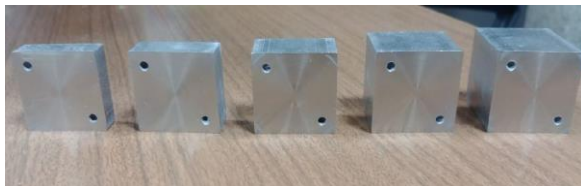

Figure 3. AISI 304 L specimens used

Sample	Size (L1xL2xs) [mm]	Uncertainty [mm]
Sample 10	30.04x30.04x9.95	0.03x0.03x0.03
Sample 14	30.01x29.98x13.90	0.04x0.02x0.05
Sample 20	30.02x29.98x19.95	0.04x0.02x0.03
Sample 28	29.98x29.97x28.07	0.05x0.03x0.08
Sample 35	29.98x29.98x35.04	0.04x0.03x0.02

Table 2. Specimens dimensions obtained with multiple caliper measurements

4.2. Operating conditions and results

For each specimen, 10 tests were carried out, for a total amount of 50 experiments. It is worth noting that the number of available equations is higher than the number of the unknown constants, thus leading to an overconstrained system. Tests were performed by varying the supplied heat power and controlling the temperature differences across the sample in the range 5-50 °C. Lower differences were avoided to preserve the good accuracy of the experimental results, whereas higher differences were not taken into account in order to keep the assumption of "local" thermal conductivity measurements. A summary of the operating conditions is given in Table 3.

Table 3. Operating conditions explored in the present experimental campaign

Sample	$\overline{T}_H - \overline{T}_C$ [°C]	Heat load Q_{el} [W]	T_{mean} [°C]
Sample 10		5.9-64.6	19.4-55.6
Sample 14		4.5-47.4	18.3-48.1
Sample 20	5-50 °C	3.2-33.8	18.4-45.9
Sample 28		2.3-24.6	18.0-43.8
Sample 35		1.9-20.1	18.2-42.4

A coarse preliminary analysis was performed to evaluate the order of magnitude of the five constants to be calibrated. According to this study, the range of variation of the desired parameters was limited to the values provided in Table 4, that shows also the iteration steps considered. According to the algorithm procedure described in the previous section, the results minimizing the computational errors are provided in Table 5.

Table 4. Iteration range and step of the constants to be calibrated

	a [W/m K]	b [W/m K^2]	U_{loss} [W/m^2 K]	R_H, R_C [m^2 K/W]
Iteration range	11-16	0.010-0.025	0.5-3	1e-6 – 4e-5
Iteration step	0.1	0.001	0.1	1e-6

Table 5. Model results and minimum *RMSE* values

Sample	a [W/m K]	b [W/m K^2]	U_{loss} [W/m^2 K]	R_H [m^2 K/W]	R_C [m^2 K/W]	RMSE [°C]
Sample 10				1.1e-5	3.3e-5	0.027
Sample 14				3.9e-5	4.0e-5	0.098
Sample 20	13.9	0.02	1	3.3e-5	2.0e-6	0.056
Sample 28				1.0e-6	3.8e-5	0.048
Sample 35				1.0e-6	1.3e-5	0.094

Once Equation (1) has been calibrated, the thermal conductivity of the samples as a function of the mean specimen temperature is shown in Figure 4, together with the total (heater and specimen) thermal losses. The experimental thermal conductivities are also compared to the reference functions given in Equations (9) and (10), providing a good agreement, with Equation (1) graphically included in both methods. Details on the assessment are provided in Table 5. No significant discrepancies are found between the different specimens analyzed. The total thermal losses, modeled as increasing functions of the temperature difference with the environment, are restrained to very low values and barely reach 2 W only when significant heat loads (more than 60 W) are applied.
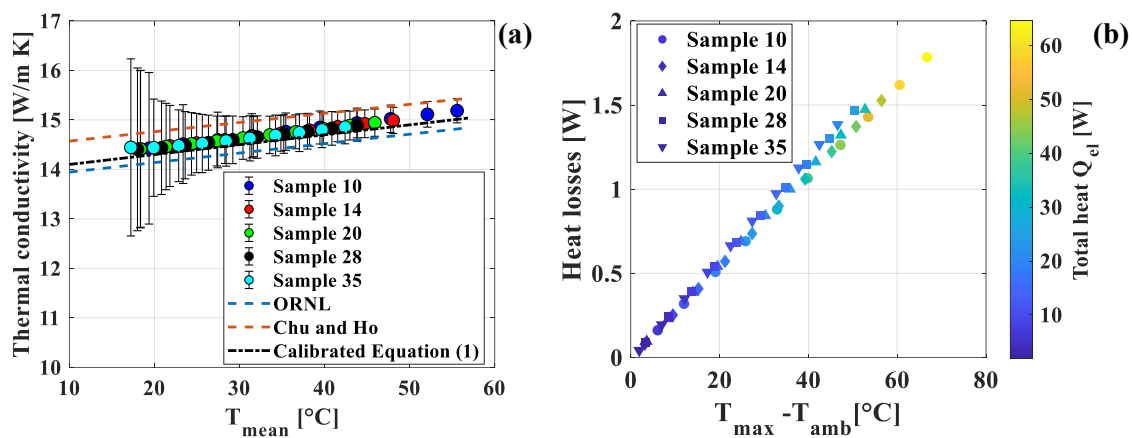

Figure 4. (a) Thermal conductivity of the AISI 304 L specimens as a function of their mean temperature; (b) Total heat losses as a function of the average temperature difference between the hot block and the ambient.

Table 5. Main assessment parameters

$RMSE_{Chu}$ [W/m K]	$RMSE_{ORNL}$ [W/m K]	$RMSE_{New\ model}$ [W/m K]	Average k uncertainty [%]	Maximum k uncertainty [%]
0.314	0.303	0.082	3.90	12.10

5. Conclusions

A testing apparatus was designed and constructed for the evaluation of the thermal conductivity of additive manufactured AM or ultra-high-temperature-ceramics UHTCs materials employed for the atmospheric entry of space vehicles.

The test facility allows the characterization of small size square (30x30 mm^2) specimens, covering a thermal conductivity measurement range between 5 and 50 W/m K. A dedicated model was developed and calibrated by taking into account the thermal losses to the surrounding environment and the contact thermal resistance between the specimens and the cold and hot sections of the test facility.

Five stainless-steel AISI 304 L specimens having thicknesses from 10 to 35 mm were tested with mean temperatures from 18.0 to 55.6 °C to validate the procedure and the performance of the apparatus. The results provided the thermal conductivity as a linear function of the mean sample temperature, according to the expression $k = 13.9 + 0.02 \cdot T$ W/m K (with T in [°C]), which is in reasonably good agreement with two reference functions available from open literature, within the operating conditions tested.

The thermal conductivity mean uncertainty goes from a maximum value of 12.1% for the lowest mean temperature of 18.0 °C to a minimum of 2.4% for the highest mean temperature of 55.6 °C. The overall calibrated thermal losses towards the ambient are estimated to be in any case lower than 2 W.

The proposed method has the advantage to allow tests on small size specimens giving as a result the k as a function of the mean temperature. This feature is interesting for R&D activities where tests on several samples produced with different mixing and processing parameters for the 3D printing process are needed. At the same time, it requires 50 measurements in different conditions and a lot of caution for the setting to limit local thermal contact resistances. This procedure therefore requires expertise and it is suggested only for research laboratory activities and not for in line checks of industrial processes.

Future plans for this project include the measurement of the thermal conductivity for a wide range commercially available UHTCs materials and 3-D printed metal items, to determine capabilities and possible limitations of this concept.

Acknowledgments

References

[1]   Buchanan C and Gardner L 2019 *Engin. Struct.* **180** 332-348
[2]   Saltzman D, Bichnevicius M, Lynch S, Simpson T, Reutzel E, Dickman C and Martukanitz R 2018 *Appl. Th. Eng.* **138** 254-263
[3]   Hwang S, Reyes E, Moon K, Rumpf R and Kim N 2014 *Electr. Mater.* **44** 771-772
[4]   Danes F, Garnier B and Dupuis T 2003 *Int. J. Thermoph.* **24** 772
[5]   Maxwell J C 1904 *Oxford: Oxford University Press* **1**
[6]   Flaata T, Michna G and Letcher T 2017 *ASME 2017 Summer HT Conference*
[7]   MATLAB 2019a Release, *Mathworks*
[8]   Moffat R J 1982 *Trans. ASME: J. Fl. Eng.* **104** 250-260
[9]   Graves R S, Kollie T G, McElroy D L and Gilchrist K E 1991 *Int. J. Thermoph.* **12** 409-415
[10]   Bogaard R H 1985 *Proc. 18th Int. Conf. Therm. Conduct., New York* 175-185
[11]   Chu T K and Ho C Y 1978 *Proc. 15th Int. Conf. Therm. Conduct., New York* 79-104